Energy & Buildings 207 (2020) 109625

Contents lists available at ScienceDirect

Energy & Buildings

journal homepage: www.elsevier.com/locate/enbuild

Printed luminescent solar concentrators: Artistic renewable energy

Jeroen ter Schiphorst[a], Marx L.M.K.H.Y.K. Cheng[b], Maxime van der Heijden[b], Renee L. Hageman[b], Emily L. Bugg[b], Teun J.L. Wagenaar[a], Michael G. Debije[b,*]

[a] Lusoco B.V., Het Kranenveld 14, 5612 AP Eindhoven, the Netherlands

[b] Laboratory of Stimuli-responsive Functional Materials and Devices, Eindhoven University of Technology, 5600 MB Eindhoven, the Netherlands

ARTICLE INFO

Article history:
Received 20 September 2019
Revised 28 October 2019
Accepted 20 November 2019
Available online 21 November 2019

ABSTRACT

The built environment and its direct surroundings show great potential for sustainable energy harvesting but often face the challenge of being integrated with solar energy generators in an aesthetically pleasing manner. In this work, we demonstrate the inkjet printing of luminescent solar concentrators with striking imagery as a promising solution where energy generation and aesthetic possibilities of transparent surfaces become possible. Inkjet printing is used to create a variety of unique patterns for enhanced aesthetics, while a model study explores the effect of patterning and use of multiple colors with this technique on the output of the device.

1. Introduction

The world is undergoing an energy transition towards smart cities with increasing interest for renewable electricity generation [1]. With the expectation that global energy consumption will only increase, new options for localized energy generation and off-grid applications are desired to reduce transport losses, ensure security of energy supply, and reduce the impact of fossil fuels on climate [2]. A major challenge in harvesting energy from renewable energy sources and integration for nearly zero-energy buildings is in simultaneously maintaining attractiveness in the appearance of the structure.

For electricity generation in urban settings, photovoltaic (PV) panels are generally employed. PVs are primarily applied on top of a roof as an add-on construction, rather than being integrated into the building façade or surroundings. With the decreasing availability of land, urban planners have responded by designing ever taller buildings, resulting in relatively small areas of rooftops for traditional PV panels but concomitant large areas of facades. Deployment of PVs in facades is challenging, since there are often both performance (non-optimal orientation, excessive shading, or increased risk of damage to the device) and aesthetic barriers to integration of traditional PV panels in buildings, although products with beautiful designs have recently become commercially available [3].

Building integrated photovoltaics (BIPV) are much in demand. Several attempts have been made to add coloration to PV cells [4–6], which show promising applicability but lack the transparency required for window applications. Transparent colored cells struggle to balance appearance, production costs and performance [7–10]. Appealing energy generation in building facades could be achieved using the luminescent solar concentrator (LSC) [11–18]. In an LSC, hidden PV cells cover only the narrow edges of a plastic or glass lightguide. By applying fluorescent coatings to the lightguide surface, both direct and indirect light is absorbed by the luminophore [19], and the emitted light redirected towards the small PV cells, which receive this concentrated light at a wavelength optimized to minimize heating effects on the PV, allowing the cells to run cooler and more efficiently (Fig. 1) [20].

Appearance is a critical factor in the application of PV systems in the built environment [21,22]. Colored glass facades are already used to create attractive buildings [23]. While transparent lightguides for use as electricity generating LSC windows have been proposed [12,15,16,24], the sunlight absorbed is generally restricted to the ultraviolet and near infrared exploitation, which necessarily limits the possible performance of the device. Recent work suggests the fractional coverage of a window by colored lightguides strongly determines whether or not the participant is comfortable with the presence of the LSC [25]. Despite introduction in the late 1970s,[26] no serious market introduction of LSC devices has yet been made. However, several efforts have addressed the potential aesthetic advantage of the LSC in building integration [17,27–30].

* Corresponding author.
E-mail address: m.g.debije@tue.nl (M.G. Debije).

https://doi.org/10.1016/j.enbuild.2019.109625
0378-7788/

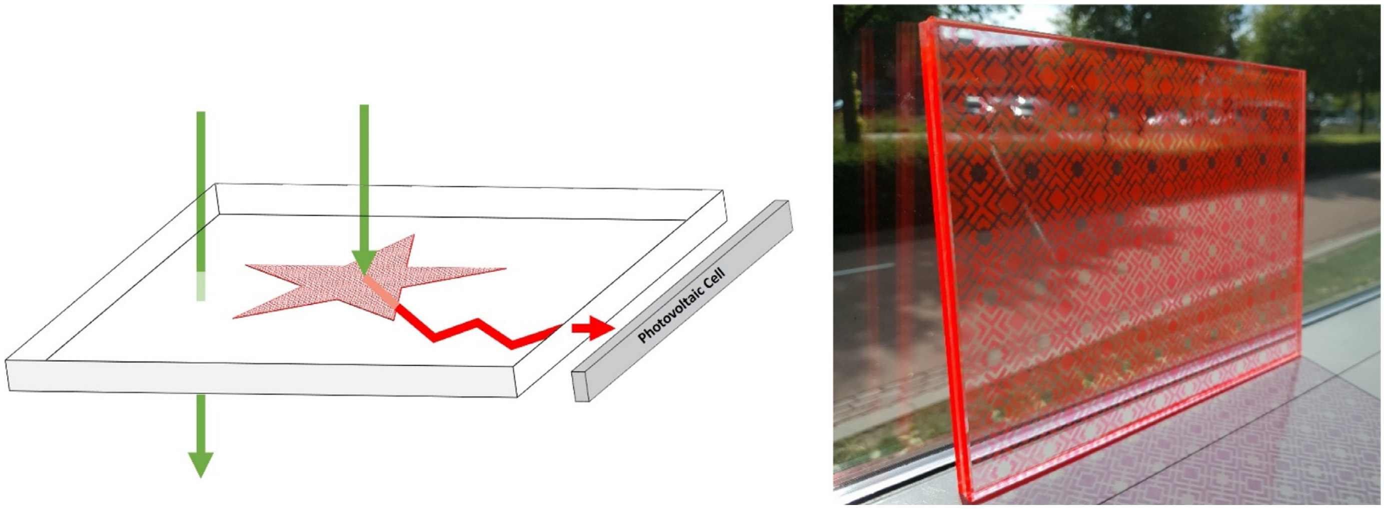

Fig. 1. (Left) Working principle of an inkjet printed luminescent solar concentrator. The fluorescent ink (red star) absorbs incident light (green arrow) and emits this by fluorescence (red arrow). Due to the difference in refractive index between the PMMA substrate and the surrounding air, a large fraction of the light is trapped inside the device and only emitted through the edges where one can attach a photovoltaic cell to generate electricity. (Right) Photograph of a printed A4 sized luminescent solar concentrator. (For interpretation of the references to color in this figure legend, the reader is referred to the web version of this article.)

There are a few reports of the patterning of the fluorescent inks for LSCs to allow color variety.[27] Most previous works generated mosaics [31], and line or grid patterns by using masks and a tedious technique of partial polymerization followed by washing away unreacted material, which besides being inefficient and making it difficult to change patterning between experiments, is also wasteful of material [32–34]. While patterning can result in a decrease in total emission due to decreased total light absorption [33,34], it could allow the device to be employed as a semi-transparent window [35], and compensate for the loss of electrical generation with beautification of the building facade [25,27]. Even though the efficiency will inferior to PV panels, the added value of LSC systems combining aesthetics with energy harvesting and possible smart sensor applications will impact the built environment for smarter energy use and monitoring of the environment without the requirement of access to power grids.

In this work, an inexpensive procedure is developed to inkjet print visually striking LSC devices that open a tremendous window of opportunity to design unique, attractive solar energy systems depicting stunning artwork that could be easily integrated in and around the modern façade, with the possibility of replacing the current printed glass for an energy harvesting solution. Inkjet patterning can deposit multiple colors with high definition and be done on demand, allowing for limitless flexibility in the design of building integrated photovoltaic systems.

2. Results and discussion

A series of 25 cm^2 devices with a variation of 12.5–100% ink surface coverage were printed (Fig. 2); the absorbance of the dye in these prints was around $A = 0.65$. The edge emissions were measured upon exposure of the surface to light from a solar simulator with the samples on a black painted metal support (Table 1). ‘Internal efficiency’ of the LSC is defined as the fraction of photons reaching the edge of the lightguide as a function of the total number of photons absorbed by the dye. ‘External efficiency’ is the fraction of photons that are emitted from the lightguide edges as a fraction of the total number of photons incident on the surface of the device from 350–1000 nm. The internal efficiency is an indication of how well the individual dyes and lightguide process the light, and the external efficiency provides a comparative performance value of the LSC device as a whole.

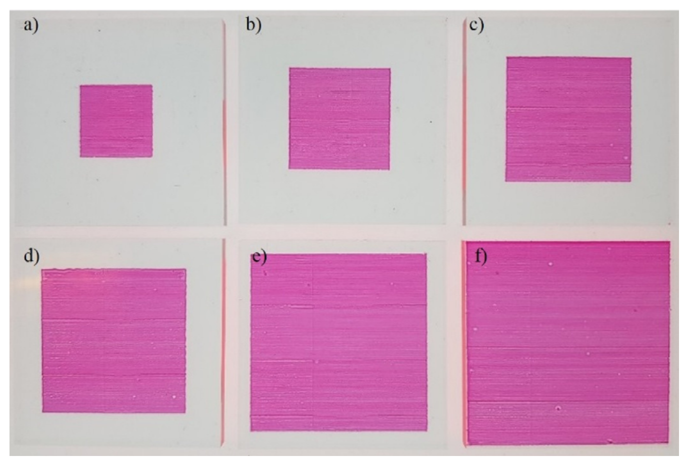

Fig. 2. Photographs of 5 × 5 cm^2 PMMA plates coated with 1% Red305 dye solutions (samples 1a–1f) with peak absorbance around 0.65.

With increasing coverage, the internal efficiency decreases, while the external efficiency increases (Table 1). Increasing coverage area of the ink results in a greater probability of reabsorption of the emitted light. These reabsorptions may result in a light loss via limited fluorescent quantum yields of the dyes, or emissions outside the ‘capture cone’ of the lightguide [14]. Both these losses reduce the internal efficiency. However, the greater coverage area also increases the absolute number of photons absorbed, which increases the absolute output of the device, despite the increase of internal losses. In a practical application, this will mean that decreasing the dye surface coverage area of the LSC will result in a non-linear reduction of electrical generation efficiency. Aesthetically appealing LSCs or devices with extensively uncovered areas for use as windows may sacrifice a fraction of the device’s external efficiency, but the increased internal efficiency will compensate to some extent.

To study the effect of different patterning designs on edge emission, eight samples were printed, each having a coverage area of 50% (Fig. 3). The photon efficiency of these devices were all found to be similar, varying between 53.4 and 60.7% (Table 2). No

Table 1
Internal and external photon efficiencies for simple centered square patterns with 12.5–100% lightguide coverage: references to Fig. 2 images of the samples are given.

Ink coverage (%)	Internal Photon Efficiency (%)	External Photon Efficiency (%)
12.5 (2a)	74.9	2.4
25.0 (2b)	62.4	3.8
37.5 (2c)	58.3	5.5
50.0 (2d)	56.7	7.0
75.0 (2e)	52.6	10.1
100.0 (2f)	48.5	12.1

Table 2
Internal and external efficiencies for complex patterns with 50% surface coverage, with reference to patterns depicted in Fig. 3.

Ink coverage (%)	Internal Photon Efficiency (%)	External Photon Efficiency (%)
50% 2 lines, 3a	55.7	8.1
50% 3 lines, 3b	54.2	8.1
50% 4 lines, 3c	55.2	8.1
50% 2 squares, 3d	53.5	7.8
50% 4 squares, 3e	58.5	8.4
50% 5 squares, 3f	56.2	8.0
50% 2 edges, 3g	53.4	7.8
50% edge square, 3h	60.7	8.7

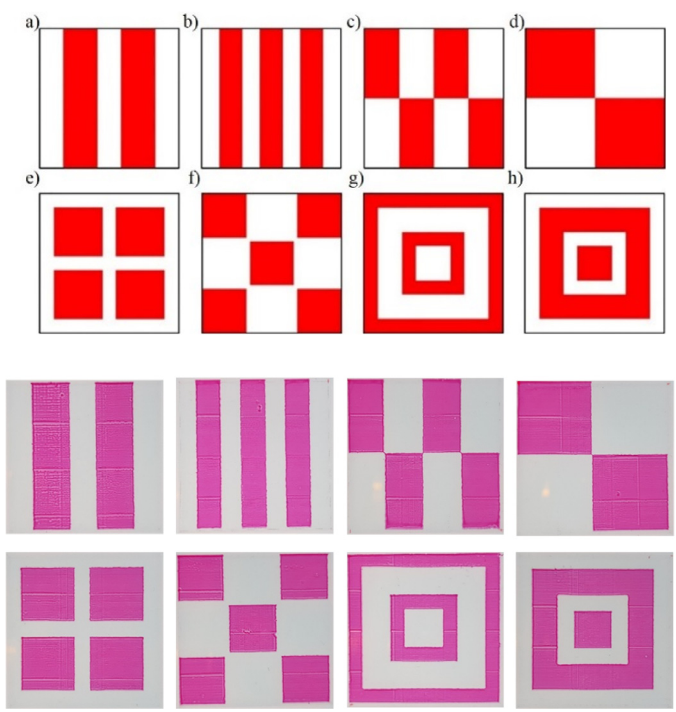

Fig. 3. Sample printed patterns of samples 3e-3l and photographs of 5 × 5 cm^2 printed devices with photographs of eight of the actual devices displayed underneath.

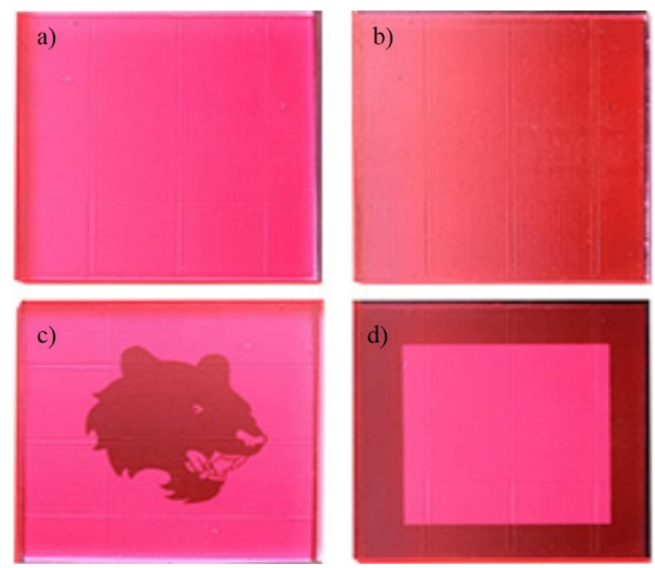

Fig. 4. a) Appearance of a printed 100% covered Red305 lightguide with peak absorbance of 0.56 covering 100% of lightguide on a uniform white paper background. b) Appearance of the same print covering 100% of lightguide on a uniform black paper background. c) Appearance of the same print on a white paper background printed with a panther image in black ink. d) Appearance of the same print on a white background with printed black edges. (For interpretation of the references to color in this figure legend, the reader is referred to the web version of this article.)

clear correlation between these patterns and edge emission were identified at the scale of the devices printed (25 cm^2).

The performance of the inkjet-printed samples were compared with samples produced earlier using the more laborious process of polymerization of a bar coated layer through a mask followed by washout procedures described in the literature [33,34]. The 100% covered inkjet printed sample with A~0.65 had an external efficiency of 12.1%, while the bar-coated, mask-polymerized sample with A~0.9 was quite comparable at ~14.8% [33] after correcting for the difference in integration ranges (350–800 nm in the current work compared to 350–750 nm in the previous work), aborbance and the lamp characteristics. Thus, the printing technique produces high-quality samples comparable to the bar coating process described in the literature.

The presence of a white scatterer at the rear side of an LSC can improve edge emissions, especially for samples of more limited size when the absorbance is limited, allowing absorption event of the otherwise unabsorbed, back scattered light [36–38]. Combining LSCs placed on top of backgrounds with printed artwork could be an engaging way to create images that actively generate electricity while simultaneously retaining their appeal as devices suitable for displaying public information or advertising, for instance. In Fig. 4, the visual Impact of modifying a rear scatterer by adding a printed panther image covering 44% of the rear surface area is shown. Including this striking image resulted in a minor decrease of only 0.7% in external efficiency compared with the pure white back-

Table 3
Internal photon efficiencies of a fully covered Red305 sample on different backgrounds.

Sample	Internal photon efficiency (%)
White background (4a)	52.2 ± 0.5
Black background (4b)	36.9 ± 0.4
Black panther background (4c)	48.2 ± 0.5
Black border (4d)	42.9 ± 0.3

Fig. 5. a) 100 × 100 × 5 mm^3 substrate patterned with ink at 15 DPI. b) 100 × 100 × 5 mm^3 patterned with ink with 15 DPI; 13 V and 15 V were used to create shadows. c) Shadow effect by using 0.5% and 1.25% Red305 dye concentrations on a 50 × 50 × 5 mm^3 substrate. (For interpretation of the references to color in this figure legend, the reader is referred to the web version of this article.)

Fig. 6. Example of a multicolor image printed on a 10 × 10 cm^2 PMMA plate using Lusoco ink containing Lumogen Red305 (red ink) and a perinone derivative (teal color) [39]. (For interpretation of the references to color in this figure legend, the reader is referred to the web version of this article.)

Table 4
Internal photon efficiencies for the LSC devices depicted in Fig. 7.

Sample	Internal Photon efficiency (%)
7a	48.2 ± 0.36
7b	9.3 ± 0.07
7c	16.0 ± 0.14
7d	20.6 ± 0.07
7e	28.0 ± 0.15
7f	18.0 ± 0.06

ground (Table 3). This shows adding significant visual enhancement of the LSCs by including easily interchangeable images on the back scattering element of the LSC can be done without severely compromising performance, perhaps even enhancing it [37]. Additional images were printed and placed behind the lightguide on white paper but no clear correlation between efficiency and placement of the figures were found. The effect of a printed image on a rear scatterer on the performance with larger scale lightguides would give insight into the advantages of the strategic placement of the ink at various positions of the device [29].

In Fig. 5, there are three examples of more striking graphic designs. These highly artistic images show the possibilities of generating a variety of patterns and tones using a single color.

These images were designed to demonstrate the unique opportunity provided by inkjet printing for LSC devices. In Fig. 5a, applying the design rules for maximum transparency while remaining a short travel distance of the light towards the edges resulted in a high resolution example. A border around the device is used to allow reduced coverage of the central area, while boosting electrical generation efficiency. Fig. 5b is created by printing the design into two parts. Here, different voltages were applied on the inkjet nozzle during printing, resulting in deposition of more ink at desired locations and showing the possibility to create a shading effect using a single ink. In this work, the neck, eyes, and nose of the face are printed with a thicker layer of ink than the side of the neck, for example. Fig. 5c is printed using two inks with different dye concentrations, showing the possibility of creating a three-dimensional effect.

The edge output of the sample shown in Fig. 5c, which has 33.5% uncoated surface, resulted in an increase of 3.3% in internal photon efficiency compared with a fully covered sample containing 1 wt.% Red305, as the higher dye concentration resulted in higher local absorbance. The geometric pattern had a decreased external efficiency since fewer photons were absorbed initially.

Naturally, the printing of images onto LSCs is not restricted to monochromatic designs [18,31,33]. A variety of colors are possible, dramatically increasing the number and types of images that could be printed (Fig. 6). The final efficiency of the device is a function of the spectral absorption, area coverage by the ink, effective overlap of absorption and emission spectra of the dyes [33], and the fluorescent quantum yields of the luminophores. When extending this to using edge attached PVs, the response of the PV and optical coupling into the solar cell are also important parameters.

To more systematically test the performance of LSCs employing multiple colors, a series of box-like patterns were printed using the Red305 dye and a perylene perinone (see Fig. 7) [39,40]. The perinone has been shown to have a somewhat lower fluorescent quantum yield than the Red305 [39]. As evidenced in Table 4, the decreased efficiency had an expected significant impact on the edge emission of the device. The selection of appropriate dyes with minimal spectral overlap and high fluorescent yields, and optimal

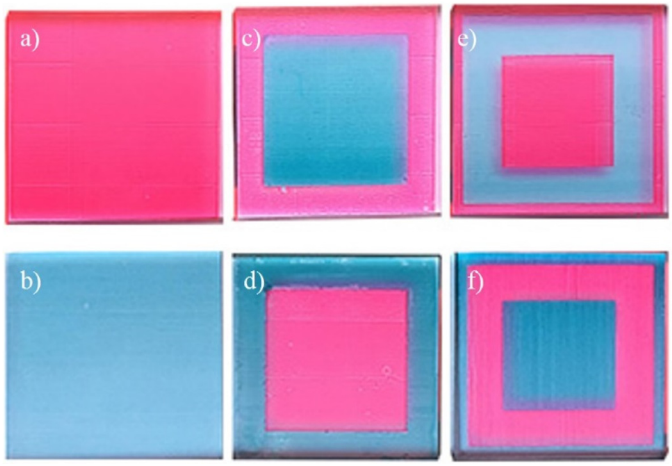

Fig. 7. Inkjet printed 5 × 5 cm^2 lightguides using inks containing two different luminophores: 1 wt% Red305 or 1 wt% of a perylene perinone [39]. (For interpretation of the references to color in this figure legend, the reader is referred to the web version of this article.)

surface distribution of dyes for multicolor images must be carefully considered if maximum efficiency is desired.

Efficiencies drop dramatically when switching to the perinone based dye, resulting in an internal photon efficiency of 9.3% (Table 4). This is a factor of 5 lower than the internal photon efficiency achieved for the equivalent fully covered lightguide printed with Red305 dye. This illustrates the importance of utilizing high quantum yield materials when introducing LSC devices into real environments.

The printing of LSCs opens many additional opportunities for light control in the device. As an example, by printing LSCs using an ink containing polymerizable liquid crystal (LC) monomers as host for the dichroic luminescent species, it is possible to align the dye molecules, gaining control over the emission directions of the light [41–45]. By directing dye emissions to specific locations along the edges of the lightguides [43] it becomes possible to employ smaller, more efficient (and expensive) PV cells.

3. Experimental

PMMA (Polymethyl methacrylate) was used as substrate (PlanoPlastics), generally 5 × 5 cm^2 or 10 × 10 cm^2 in size. On top of the substrate the dye ink was printed by an inkjet printer. The ink mixture (Lusoco B.V.) contains either a red perylene based dye, Lumogen Red305 (BASF) [46,47], or a perylene perinone [39].

Printing of the ink was performed using a Dimatrix DMP-2850 equipped with a cartridge containing 2 ml of the mixture (10 pl drop volume). The head of the cartridge was heated to 50 °C with a meniscus set point of 1.0 mbar and printing was performed operating the piezo elements at 16 V. During printing the cartridge was purged every 120 s for 0.3 s and wiped to keep the nozzle plate clean. The cartridge was covered by aluminum foil to prevent the ink from polymerizing during printing. During the printing, a LED lamp (Thor Labs 365 nm LED, including a collimator to adjust the spot size and intensity) was used to pin the ink in position. After printing, the substrate was transferred to an N_2 environment and further polymerized for 30 s with an 8 mW/cm^2 TL beam (15 W Philips CLEO (Hg); Hevlar 50 Hz 230 V), to further cure the ink. Images were created by loading a BMP file into the controlling computer with a resolution of 1693 pixels/inch so that the image is printed with a droplet spacing of 15 DPI.

The LSC edge-emission was measured by exposing the sample placed on a black-painted metal support shelf from the top of the waveguide with a 300 W AM1.5 solar simulator light source (Lot Oriel Group). The photon output at the edges of the PMMA was detected by integrating sphere (LMS-100, Labsphere) with a diode array detector (RPS900, Internal Light) with a wavelength range of 350–1000 nm. The transmission spectra through the LSC was measured by a spectrometer (Perkin Elmer Lambda 750) over a spectral range of 350–800 nm with a Perkin Elmer 150 mm integrating sphere detector (lead sulfide (PbS) combined with a photon multiplier tube (PMT).

The edge emissions of the four edges of the LSC lightguide were measured, summed, and the photon output, n, calculated from:

$$nE_{photon} = \frac{hc}{\lambda} \tag{1}$$

where h is the Planck constant, c the speed of light, λ is the wavelength (m), and E_{photon} the energy of a single photon.

The energy absorbed by the dyes, E_{abs}, was estimated by multiplying the measured lamp spectra by the absorption spectra of the dye for the 25 cm^2 samples, adjusted for the fractional coverage of the dyes calculated from the BMP drawing. The internal photon efficiency, η_{in}, is obtained by:

$$\eta_{in} = \frac{Photons_{out}}{Photons_{abs}} \tag{2}$$

where the number of photons absorbed, $photons_{abs}$ were summed over the range of 380–800 nm and the number of edge emitted photons $photons_{out}$ for the wavelength range of 500–800 nm for the Red305 dye and 550–850 nm for the perylene perinone dye.

The external efficiency, η_{ext}, is calculated by:

$$\eta_{ext} = \frac{Photons_{out}}{Photons_{incident}} \tag{3}$$

where the $photons_{in}$ and $photons_{out}$ were summed over the appropriate wavelength range.

4. Conclusions

In this work, it is shown that by inkjet printing fluorescent ink on a waveguide, LSCs can be designed that can not only generate electricity, but also show dramatically improved aesthetic possibilities for BIPV. These devices are expected to have a strong visual impact when integrated within building envelopes for enhanced aesthetics and add to the options when working towards (near)-zero energy emission buildings. The images presented in this work show the possibility of creating 3D effects by adjusting either the quantity of ink on the lightguide surface or the amount of chromophore present in the ink within single color prints and the generation of multicolor images via the use of multiple dye molecules, thus boosting their appeal for integration into the urban environment. The true potential of these devices will become obvious when a combination of invisible inks (UV, IR) and different colors are combined to achieve both maximal energy generation and visual effects.

Declaration of Competing Interest

Jeroen ter Schiphorst and Teun Wagenaar acknowledge being the founders of Lusoco B.V., which intends to commercialize the technology.

Acknowledgements

The authors would like to thank Dr. Johan Lub for his insightful discussions.

References

[1] O. Inganäs, V. Sundström, Solar energy for electricity and fuels, Ambio 45 (2016) 15–23 (S1).
[2] P.A. Owusu, S. Asumadu-Sarkodie, A review of renewable energy sources, sustainability issues and climate change mitigation, Cogent Eng. 3 (1) (2016) 1167990.
[3] For example, https://kameleonsolar.com/ and https://studio-solarix.nl/ (accessed Sept. 11, 2019).
[4] E. Klampaftis, D. Ross, G. Kocher-Oberlehner, B.S. Richards, Integration of color and graphical design for photovoltaic modules using luminescent materials, IEEE J. Photovoltaics 5 (2) (2015) 584–590.
[5] G. Peharz, K. Berger, B. Kubicek, M. Aichinger, M. Grobbauer, J. Gratzer, W. Nemitz, B. Großschädl, C. Auer, C.;. Prietl, et al., Application of plasmonic coloring for making building integrated pv modules comprising of green solar cells, Renew. Energy 109 (2017) 542–550.
[6] D. Liu, L. Wang, Q. Cui, L.J. Guo, Planar metasurfaces enable high-efficiency colored perovskite solar cells, Adv. Sci. 5 (10) (2018) 1800836.
[7] A.A.F. Husain, W.Z.W. Hasan, S. Shafie, M.N. Hamidon, S.S. Pandey, A review of transparent solar photovoltaic technologies, Renew. Sustain. Energy Rev. 94 (2018) 779–791.
[8] V. Vohra, Can polymer solar cells open the path to sustainable and efficient photovoltaic windows fabrication? Chem. Rec. 19 (7) (2019) 1166–1178.
[9] D. Yang, T. Sano, H. Sasabe, L. Yang, S. Ohisa, Y. Chen, Y. Huang, J. Kido, Colorful squaraines dyes for efficient solution-processed all small-molecule semitransparent organic solar cells, ACS Appl. Mater. Interfaces 10 (31) (2018) 26465–26472.
[10] N. Dhindsa, J. Walia, S.S. Saini, A platform for colorful solar cells with enhanced absorption, Nanotechnology 27 (49) (2016) 495203.
[11] B. McKenna, R.C. Evans, Towards efficient spectral converters through materials design for luminescent solar devices, Adv. Mater. 29 (28) (2017) 1606491.
[12] Y. Zhao, G.A. Meek, B.G. Levine, R.R. Lunt, Near-Infrared harvesting transparent luminescent solar concentrators, Adv. Opt. Mater. 2 (7) (2014) 606–611.
[13] W.G.J.H. Van Sark, K.W.J. Barnham, L.H. Slooff, A.J. Chatten, A. Büchtemann, A. Meyer, S.J. McCormack, R. Koole, D.J. Farrell, R. Bose, et al., Luminescent solar concentrators - a review of recent results, Opt. Express 16 (26) (2008) 21773.
[14] M.G. Debije, P.P.C. Verbunt, Thirty years of luminescent solar concentrator research: solar energy for the built environment, Adv. Energy Mater. 2 (1) (2012) 12–35.
[15] O.M. ten Kate, K.W. Krämer, E. van der Kolk, Efficient luminescent solar concentrators based on self-absorption free, tm 2+ doped halides, Sol. Energy Mater. Sol. Cells 140 (2015) 115–120.
[16] M.G. Debije, Solar energy collectors with tunable transmission, Adv. Funct. Mater. 20 (9) (2010) 1498–1502.
[17] A. Reinders, R. Kishore, L. Slooff, W. Eggink, Luminescent solar concentrator photovoltaic designs, Jpn. J. Appl. Phys. 57 (8) (2018) 1–10.
[18] A. Reinders, M.G. Debije, A. Rosemann, Measured efficiency of a luminescent solar concentrator pv module called leaf roof, IEEE J. Photovoltaics 7 (2017) 1663–1666.
[19] M.G. Debije, V.A. Rajkumar, Direct versus indirect illumination of a prototype luminescent solar concentrator, Sol. Energy 122 (2015) 334–340.
[20] V.A. Rajkumar, C. Weijers, M.G. Debije, Distribution of absorbed heat in luminescent solar concentrator lightguides and effect on temperatures of mounted photovoltaic cells, Renew. Energy 80 (2015) 308–315.
[21] S. Lien, Artist photovoltaic modules, Energies 9 (7) (2016) 551.
[22] B. Petter Jelle, C. Breivik, H. Drolsum Røkenes, Building integrated photovoltaic products: a state-of-the-art review and future research opportunities, Sol. Energy Mater. Sol. Cells 100 (2012) 69–96.
[23] S.M. Hosseini, M. Mohammadi, A. Rosemann, T. Schröder, Quantitative investigation through climate-based daylight metrics of visual comfort due to colorful glass and orosi windows in iranian architecture, J. Daylighting 5 (2) (2018) 21–33.
[24] M. Fathi, M. Abderrezek, F. Djahli, Experimentations on luminescent glazing for solar electricity generation in buildings, Optik 148 (2017) 14–27.
[25] F.M. Vossen, M.P.J. Aarts, M.G. Debije, Visual performance of red luminescent solar concentrating windows in an office environment, Energy Build. 113 (2016) 123–132.
[26] W.H. Weber, J. Lambe, Luminescent greenhouse collector for solar radiation, Appl. Opt. 15 (10) (1976) 2299–2300.
[27] A. Renny, C. Yang, R. Anthony, R.R. Lunt, Luminescent solar concentrator paintings: connecting art and energy, J. Chem. Educ. 95 (7) (2018) 1161–1166.
[28] M. Kanellis, M.M. de Jong, L. Slooff, M.G. Debije, The solar noise barrier project: 1. effect of incident light orientation on the performance of a large-scale luminescent solar concentrator noise barrier, Renew. Energy 103 (2016) 647–652.
[29] M.G. Debije, C. Tzikas, V.A. Rajkumar, M.M. de Jong, M. M.de Jong, The solar noise barrier project: 2. the effect of street art on the performance of a large scale luminescent solar concentrator prototype, Renew. Energy 113 (2017) 1288–1292.
[30] A. Kerrouche, D.A. Hardy, D. Ross, B.S. Richards, Luminescent solar concentrators: from experimental validation of 3D ray-tracing simulations to coloured stained-glass windows for bipv, Sol. Energy Mater. Sol. Cells 122 (0) (2014) 99–106.
[31] W. van Sark, P. Moraitis, C. Aalberts, M. Drent, T. Grasso, Y. L'Ortije, M. Visschers, M. Westra, R. Plas, W. Planje, The "Electric Mondrian" as a luminescent solar concentrator demonstrator case study, Sol. RRL 1 (2017) 1600015 (3–4).
[32] A.M. Kendhale, A.P.H.J. Schenning, M.G. Debije, Superior alignment of multi--chromophoric perylenebisimides in nematic liquid crystals and their application in switchable optical waveguides, J. Mater. Chem. A 2 (2013) 229–232.
[33] P.T.M. Albers, C.W.M. Bastiaansen, M.G. Debije, Dual waveguide patterned luminescent solar concentrators, Sol. Energy 95 (2013) 216–223.
[34] S. Tsoi, D.J. Broer, C.W.M. Bastiaansen, M.G. Debije, Patterned dye structure limit reabsorption in luminescent solar concentrators, Opt. Express 18 (2010) A536–A543.
[35] D. Shin, S.-H. Choi, Recent studies of semitransparent solar cells, Coatings 8 (10) (2018) 329.
[36] M.G. Debije, M.-.P. Van, P.P.C. Verbunt, D.J. Broer, C.W.M. Bastiaansen, The effect of an organic selectively-reflecting mirror on the performance of a luminescent solar concentrator, in: 24th European Solar Energy Conference, 93, Hamburg, Germany, 2009, pp. 373–376. Vol.
[37] M.G. Debije, W. Dekkers, Functionalizing the rear scatterer in a luminescent solar concentrator, J. Renew. Sust. Energy 4 (2012) 13103.
[38] L.H. Slooff, E.E. Bende, A.R. Burgers, T. Budel, M. Pravettoni, R.P. Kenny, E.D. Dunlop, A. Büchtemann, A luminescent solar concentrator with 7.1% power conversion efficiency, Phys Status Solidi - R 2 (6) (2008) 257–259.
[39] M.G. Debije, P.P.C. Verbunt, P.J. Nadkarni, S. Velate, K. Bhaumik, S. Nedumbamana, B.C. Rowan, B.S. Richards, T.L. Hoeks, Promising fluorescent dye for solar energy conversion based on a perylene perinone, Appl. Opt. 50 (2) (2011) 163–169.
[40] L. Desmet, A.J.M. Ras, D.K.G. De Boer, M.G. Debije, Monocrystalline silicon photovoltaic luminescent solar concentrator with 4.2% power conversion efficiency, Opt. Lett. 37 (2012) 3087–3089.
[41] P.P.C. Verbunt, A. Kaiser, K. Hermans, C.W.M. Bastiaansen, D.J. Broer, M.G. Debije, Controlling light emission in luminescent solar concentrators through use of dye molecules planarly aligned by liquid crystals, Adv. Func. Mater. 19 (2009) 2714–2719.
[42] P.P.C. Verbunt, T.M. de Jong, D.K.G. de Boer, D.J. Broer, M.G. Debije, Anisotropic light emission from aligned luminophores, Eur. Phys. J. Appl. Phys. Appl. Phys. 67 (01) (2014) 10201.
[43] B.J. Bruijnaers, A.P.H.J. Schenning, M.G. Debije, Capture and concentration of light to a spot in plastic lightguides by circular luminophore arrangements, Adv. Opt. Mater. 3 (2) (2015) 257–262.
[44] C.L. Mulder, P.D. Reusswig, A.M. Velázquez, H. Kim, C. Rotschild, M.A. Baldo, Dye alignment in luminescent solar concentrators: I. vertical alignment for improved waveguide coupling, Opt. Express 18 (2010) A79–A90 (S1).
[45] C.L. Mulder, P.D. Reusswig, A.P. Beyler, H. Kim, C. Rotschild, M.A. Baldo, Dye alignment in luminescent solar concentrators: II. horizontal alignment for energy harvesting in linear polarizers, Opt. Express 18 (9) (2010) A91–A99.
[46] G. Seybold, G. Wagenblast, New perylene and violanthrone dyestuffs for fluorescent collectors, Dye. Pigm. 11 (1989) 303–317.
[47] L.R. Wilson, B.S. Richards, Measurement method for photoluminescent quantum yields of fluorescent organic dyes in polymethyl methacrylate for luminescent solar concentrators, Appl. Opt. 48 (2) (2009) 212–220.